Self-Assembling Characteristics of A New Nonionic Gemini Surfactant

Ramya Santhana Gopala Krishnan,[†] Sathiah Thennarasu,[‡] and Asit Baran Mandal*[,†]

Chemical Laboratory and Organic Chemistry Division, Central Leather Research Institute, Adyar, Chennai-600020, India

Received: November 21, 2003; In Final Form: April 10, 2004

A new class of unusual nonionic gemini surfactant, viz. the bis-amide *p*-phenylenediamine Boc-bis-glycamide, was synthesized for the first time in our laboratory. The bis-amide is insoluble in water. However, the evidence for micelle formation of this bis-amide in chloroform has been obtained from surface tension, Langmuir film balance, and UV−visible, IR, and fluorescence spectroscopy. The critical micelle concentration (cmc) of this bis-amide, obtained by these techniques, correlates well. Tensiometry gave the cmc value, surface activity, and Gibbs molecular surface area. Film studies on the bis-amide gemini gave limiting areas and collapse pressures. The results of film studies also suggest that the bis-amide forms a stable monolayer film even at low concentrations and the limiting areas obtained at high concentrations (above the cmc value) are in good agreement with the contact area estimated from the theoretically calculated Connolly surface treatments. Both theoretical and experimental results suggest that the bis-amide molecules at high concentrations (above the cmc value) prefer slightly tilted conformations rather than a fully extended conformation at the air/water interface. The aggregation numbers of the bis-amide have also been determined by using both steady-state and time-resolved fluorescence methods, and they are in good agreement with each other. The concentration dependence aggregation number for bis-amide micelles has also been observed, and the results suggest the formation of only small micelles, despite the potential to grow; this is similar to the case for many micellar geminis. Computer simulation techniques show that about 11 molecules of bis-amide can aggregate to form a cluster. The IR spectra of the bis-amide in pre- and postmicellar regions were analyzed; there is no significant change in the intensity of the intermolecular hydrogen-bonding pattern for the bis-amide in the monomeric and micellar states. However, the intensity of the solvent-exposed −N−H stretching band increased as a function of bis-amide concentration after the cmc value was obtained. The fluorescence intensity of ANS in chloroform increases on interaction with bis-amide micelles, suggesting that, even in apolar media, ANS binds to the bis-amide in a region of lower polarity than does the chloroform alone. The pyrene emission intensity ratio of the first vibronic band to the third band as a function of bis-amide concentration suggested the hydrophobic character of bis-amide micelles in chloroform. Since there is no trace amount of water present in the system and the aggregate formation of the bis-amide is in the presence of pure chloroform solvent only, the species may be considered an inverted micelle. Steady-state fluorescence results suggest that 66% of the total pyrene emission is accessible to quenching in bis-amide micelles in chloroform. On the basis of lifetime measurements, the bimolecular quenching rate constant of the pyrene by CPC quencher in bis-amide micelles was found to be $(1.4 \pm 0.3) \times 10^7$ M^{-1} s^{-1}, which is due to collisional quenching by strongly partitioning quenchers.

Introduction

Gemini surfactants are a kind of surfactant molecule consisting of a short hydrocarbon spacer that connects two polar headgroups. As a result, the headgroups are held at a shorter distance, so that the assembly of these surfactants results in remarkable changes in the physicochemical properties of the aggregates.[1,2] Aggregation of these surfactants in solutions is valuable in modeling some interactions. These interactions have been used to discover novel materials. Moreover, they have attracted a great deal of attention in the area of surfactant research because of their many unusual properties.[3−5] They pack efficiently into micelles, giving very low values of critical micelle concentration (cmc). A direct consequence of the presence of two hydrophobic tails in gemini surfactants is a sharp and uniform decrease in cmc values.[6,7] We have synthesized a new bis-amide compound, viz. *p*-phenylenediamine Boc-bis-glycamide, which has a structure similar to that of a nonionic gemini surfactant. It has a complex arrangement of hydrophobic and hydrophilic segments. The *p*-phenylenediamine group is considered to be a spacer group that connects two amide functional headgroups with the hydrophobic moieties; hence, the molecule has been considered to be a double-head−double-tail gemini surfactant. The structure of the bis-amide compound is shown in Figure 1. Normally, nonionic gemini surfactants aggregate as vesicles. However, most of the biologically significant surfactants aggregate as micelles when the hydrocarbon chain length is reasonably large and the electrostatic repulsions between the headgroups are weak. In 1993, Menger et al.[3a] mentioned that "it is becoming more and more difficult to extract fundamentally new structural information on conventional micellar systems". Two strategies are available to

* To whom correspondence should be addressed. Fax: + 91-44-24911589. Tel: +91-44-24911386/24411630. E-mail: abmandal@hotmail.com; clrichem@mailcity.com.

[†] Chemical Laboratory.

[‡] Organic Chemistry Division.

10.1021/jp037554j CCC: $27.50
Published on Web 05/27/2004

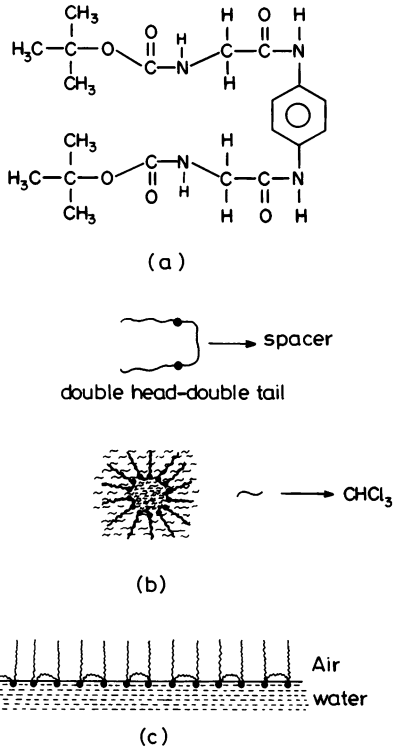

Figure 1. (a) Structure of *p*-phenylenediamine Boc-bis-glycamide. (b) Micelle pattern of bis-amide molecules in chloroform. (c) Monolayers of bis-amide molecules at the air/water interface.

counter this problem: (i) one can develop (or wait for) new instrumentation to spur further research in the area, and (ii) one can synthesize some surfactants, especially ones with unusual structural elements, and then investigate how these modifications affect the self-assembling process. One decade has already passed, and as we are somewhat impatient and have observed the advent of synthetic organic chemistry including physical chemistry aspects, we chose the latter approach. This preference has given rise to the current paper. In 1993, Menger et al.[3] had also expressed some concern at the beginning that their synthesized long-chain hydrophobic gemini surfactants with rigid spacers might not dissolve in water. However, initial tests proved otherwise, and they prepared a series of cationic and anionic geminis and reported on their properties. We have concerns similar to those of Menger et al.[3] However, our concern still persists, because our synthesized bis-amide nonionic gemini surfactant is insoluble in water and soluble in chloroform. Moreover, the micelle formation of amphipathic molecules in apolar solvents has been debated in the past because the plot of optical properties vs amphipathic concentration is not sharp enough to get a clear break point, and as a result, this gives variable cmc values. In the recent past,[8d,e] we have demonstrated that the Boc-Val-Val-Ile-OMe tripeptide found in parallel β-sheets of triosephosphate isomerase forms micelles in an apolar medium such as chloroform. Evidence for this was obtained by using UV−visible, fluorescence, IR, and NMR spectroscopy,[8d,e] where clear break points were observed. Conformational analysis[8d] of the above tripeptide in chloroform has been carried out using the nuclear Overhauser effect (NOE), and these NMR results suggested an extended structure for the tripeptides in chloroform. We have also carried out aggregation, hydrogen-bonding, and thermodynamic studies on the above tripeptide micelles in chloroform.[8e] We have demonstrated the self-assembling properties of many surfactants, polymers, peptides, and collagens in aqueous and nonaqueous media.[8−12] The aggregation behavior of some gemini surfactants and their interactions with polymers and triblock copolymers in aqueous solutions in light of the thermodynamic studies have recently been studied by Wettig et al.[13a−d] The following aspects of nonionic heterogemini (HG) surfactants were reported recently in the Ph.D. thesis of Alami.[13e] The synthetic route, the aggregation behavior, the adsorption at the air−water and solid−water interfaces, the micelle microstructure, micelle dynamics, micelle solubilization, and interactions with other surfactants have been studied.[13e] Therefore, with these motivations, in this paper we report for the first time an interesting study of an unusual micelle-forming nonionic Gemini surfactant, viz. a bis-amide in chloroform, using various experimental techniques and theoretical computational methods with the fond hope of stimulating further research.

Experimental Section

Synthesis, Purification and Characterization of *p*-Phenylenediamine Boc-bis-glycamide. The symmetric anhydride of Boc-glycine was prepared using 0.02 equiv of Boc-glycine and 0.01 equiv of dicyclohexylcarbodiimide (DCCI) in 25 mL of dry 1,2-dichloromethane at 5 °C. The dicyclohexylurea that formed was filtered off, and the clear solution was placed in a round-bottom flask equipped with a stirrer and a dropping funnel. *p*-Phenylenediamine (500 mg; 0.005 mol) was dissolved in 20 mL of dry dichloromethane contained in the separating funnel. *p*-Phenylenediamine was added dropwise at room temperature to the stirred solution of symmetric anhydride. Within a few minutes, a pale brown precipitate was formed. After 45 min, the precipitate that formed was collected and washed extensively with dichloromethane. The solid obtained was dissolved in methanol and triturated with 50% saturated bicarbonate solution. Finally, the sample was characterized by various spectroscopic techniques. Spectral data are as follows. IR (KBr): 3421, 3324, 3182, 3106, 2974, 2929, 2850, 1687, 1624, 1587, 1505, 1407, 1368, 1240, 1167, 1058 cm^{-1}. ^1H NMR: δ (ppm) 9.87 (s, 2H, NH), 7.51 (s, 4H), 7.02 (t, 2H, NH) 3.70 (d, 4H), 1.40 (s, 18H). ^{13}C NMR: δ (ppm) 167.6, 155.6, 134.0, 119.2, 43.4, 33.0, 27.9. MS: *m*/*z* 422 (M^+), 405, 367, 327, 281, 207, 147, 105, 97, 91, 82, 73. Anal. Found: C, 57.23; H, 6.9; N, 13.09. Calcd: C, 56.87; H, 7.10; N, 13.27.

Materials. All the reagents used in the experiments were of analytical grade. HPLC grade chloroform was used for all the experiments. Pyrene and 8-anilino-1-naphthalenesulfonic acid (ANS) were purchased from Fluka and were used after recrystallization. *N*-Cetylpyridinium chloride (CPC) was obtained from Sigma and was purified by recrystallizing twice from an acetone−ethanol mixture and drying in a vacuum oven at 60 °C.

Spectral Studies. UV−visible and steady-state fluorescence measurements were made on a Shimadzu UV-160A spectrometer and Hitachi Model No. 650-40 fluorimeter, respectively. UV−visible spectra for various concentrations of bis-amide were recorded in the wavelength range 200−300 nm to determine the critical micelle concentration. In the case of fluorescence experiments, pyrene and ANS were used as external probes, since the bis-amide contains no fluorescence excited state. The emission intensities of pyrene in different concentrations of bis-amide solutions were recorded by exciting the sample at 320 nm.

Time-Resolved Fluorescence Experiments. Fluorescence decay curves and lifetime measurements were carried out using a time-correlated single-photon counting (TCSPC) spectrofluorimeter (IBH, Model 5000U). The excitation source was a 5000f coaxial flash lamp operated at a frequency of 100 kHz; the pulse

width of the lamp under the operating conditions used was 1.2−1.5 ns full width half-maximum (fwhm), using nitrogen at a pressure of 1 bar. The fluorescence emission was monitored at right angles to the excitation path, and photons were detected by a MCP-PMT (Hamamatsu, Model R3809U-50) detector. The lifetimes were estimated from the measured fluorescence decay curves and were analyzed using a nonlinear least-squares iterative fitting procedure. We have described the details regarding time-resolved fluorescence experiments in our recent publications.[14]

Surface Tensiometry. Surface tension measurements were performed on an EZ-Tensiometer Model No. 201 apparatus with a 6 cm Pt/Ir ring. Milli-Q water of specific conductance 2−3 μS cm^{-1} was used for all sample preparations. Solutions were equilibrated for 1 h before taking measurements. Extra care was taken to avoid disturbing the interface during measurements.

Monolayer Experiments. The surface pressure−molecular area ($\pi-A$) isotherms were performed on a NIMA Technology Ltd. Model 611 single-barrier trough at a continuous compression rate of 150 cm^2 min^{-1}. In all experiments, using a Langmuir film balance, $\pi-A$ isotherms were measured after confirmation of purity of the water from the surface tension value (71.5−72 mN/m) at 22 °C and the absence of any surface-active impurity in the solvent by a blank run on water using solvent alone. In all these experiments, water and the solvent were found to be free from such impurities. Deionized, doubly distilled water from a Milli-Q system (Millipore) was used as the subphase. The pure water subphase was kept at a temperature of 22 ± 0.2 °C. The monolayers (thin films) of bis-amide were obtained by spreading 100 μL of bis-amide solution in chloroform using a Hamilton syringe on the surface of the water. The film was subsequently allowed to dry for 5 min in order to complete the removal of chloroform. The $\pi-A$ isotherms were recorded for bis-amide solutions of various concentrations. All the $\pi-A$ isotherm measurements were repeated three times, yielding reproducible results. We have described details regarding the monolayer experiments in our recent publications.[11e,f]

Computational Methods. For calculation of the surface area, the model of the bis-amide molecule is made using a builder package of the Cerius^2 molecular simulation package. The geometry of the molecule is minimized using a universal force field employing the energy minimizer module of the Cerius^2 package. The geometry corresponding to the minimum energy has been used to calculate the Connolly surface area of the bis-amide molecule. The contact, saddle, concave, and total Connolly surface areas have been computed. Computational details have been described in earlier publications.[15]

Results and Discussion

Critical Micelle Concentration of Bis-Amide in Chloroform and Hydrogen Bonding. The bis-amide molecule shows an absorption maximum at 266 nm due to the presence of an aromatic group in its structure. The critical micelle concentration (cmc) was determined by using the conventional methods, where absorbance or emission intensity is plotted as a function of concentration of bis-amide. The abrupt change in the slope of the plots was considered to be the cmc (Figure 2). The plot of absorbance vs concentration of bis-amide is shown in Figure 2. Since the bis-amide molecule does not contain any fluorescent excited state, pyrene is used as an external probe in fluorescence experiments. Curve 2 of Figure 2 shows the emission intensity ratio of the first vibronic band to the third band (i.e., I_1/I_3) as a function of bis-amide concentration for a fixed concentration of pyrene (1 μM). The abrupt decrease of I_1/I_3 upon increasing

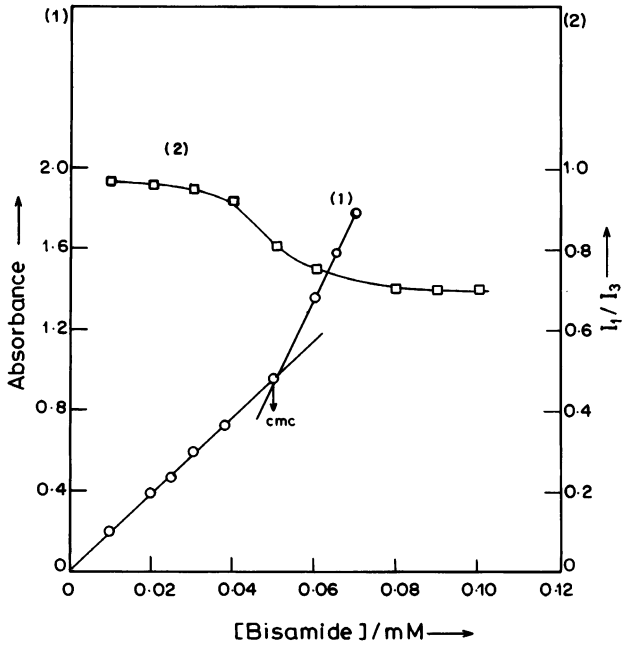

Figure 2. Plots of absorbance (in the absence of pyrene) and the ratio of emission intensities of the first and third peaks of pyrene: i.e., I_1/I_3 vs concentrations of bis-amide in chloroform at 22 °C. Conditions: [pyrene] = 1 μM (fixed); λ_{ex} 320 nm; λ_{em} 374 and 387 nm. Curve numbers correspond to ordinate scale numbers.

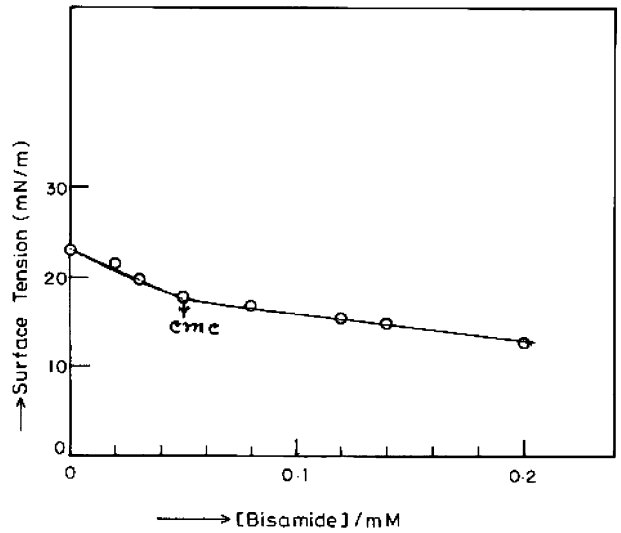

Figure 3. Plot of surface tension vs various concentrations of bis-amide at 22 °C.

the concentration of bis-amide occurs over the range of concentration 0.04−0.05 mM, which defines the cmc region. Although the question of micelle formation in apolar solvents was debated in many cases, the aggregation behavior of bis-amide molecules in chloroform has been explained in the present study and also substantiated by surface tension measurements (Figure 3) and ANS emission intensities (Figure 4). We have observed that the fluorescence emission intensity of ANS in chloroform increases upon interaction with bis-amide micelles, suggesting that, even in apolar media, ANS binds to the bis-amide in the region (either inside or in the interfacial region of the micelles[16]) of lower polarity than the chloroform alone. The fluorescence emission spectra of ANS in chloroform in the absence and presence of various concentrations of bis-amide are shown in Figure 4. It should be noted that there is no shift in the ANS emission wavelength in the presence of bis-amide, owing[8b,16] to the decrease in polarity as well as the unaltered

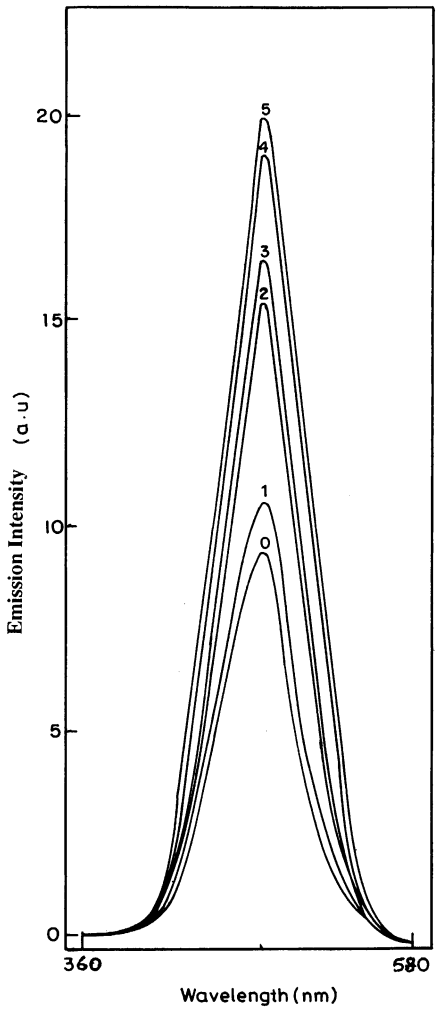

Figure 4. Fluorescence spectra of ANS in chloroform at various concentrations of bis-amide at 22 °C. Conditions: [ANS] = 1×10^{-6} M (fixed); λ_{ex} 346 nm; λ_{em} 480 nm. Curves 0−5: (0, 1, 4, 6, 8, 10) × 10^{-5} M bis-amide, respectively.

microviscosity of the environment.[8b,16] The reported surface tension value for chloroform is around 25 mN/m at 22 °C. However, the surface tension value of bis-amide in chloroform decreases with an increase in concentration of bis-amide, even reaching 14 mN/m at 0.2 mM bis-amide concentration. The surface tension values are similar to those of alkanes, and hence, the bis-amide micellar system behaves like highly nonpolar solvents. Also, there have been reports on the very low values of surface tension for gemini surfactants at the critical micelle concentration.[3−7] Hence, the orientation of bis-amide micelles may be such that the *p*-phenylenediamine spacer groups come closer together because of strong $\pi-\pi$ interactions between them to a form micellar inner core, whereas the bulky *tert*-butyloxycarbonyl tail groups (Boc) point toward the outside. The closer proximity of bulky Boc groups might be prevented due to steric hindrance. The fluorescence and surface tension results suggest that the bis-amide molecule is hydrophobic overall, and hence, the affinity between the hydrophilic groups is considered to be insignificant. However, the solvophobic −NH−CO− is thought to be hydrogen bonded intermolecularly in a low dielectric medium.[17] The possibility of intramolecular hydrogen bonding might also be the reason to make the molecules come closer together to give a compact structure for bis-amide micelles. The formation of hydrogen bonding was also confirmed by the FTIR measurements of various concentrations of bis-amide micelles in chloroform (Figure 5). The NH stretching region of the IR

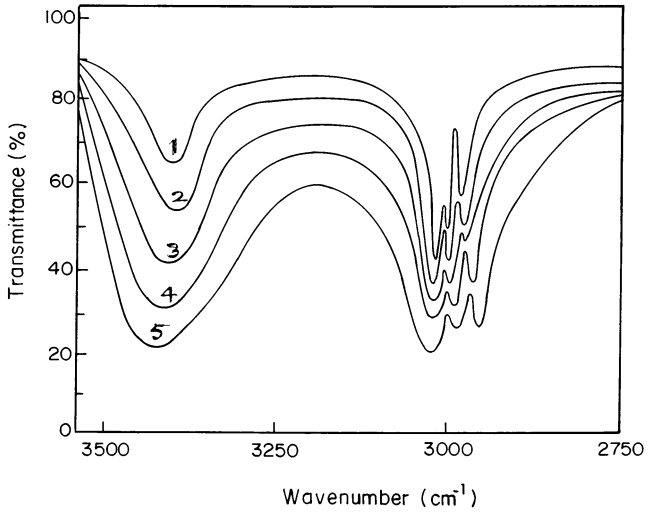

Figure 5. IR spectra of bis-amide in chloroform at various concentrations at 22 °C. Curves 1−5: (1, 2, 4, 6, 8) × 10^{-5} M bis-amide, respectively.

spectra of the bis-amide shows two absorption peaks: one at 3420 cm^{-1} is attributed to the presence of a solvated N−H, and the other at 3070 cm^{-1} may be due to the intermolecularly H-bonded N−H groups.[18] The IR spectra show that hydrogen bonding occurs even at premicellar levels of the bis-amide in chloroform, and the broadening of the peaks reveals the formation of hydrogen bonds in chloroform (Figure 5). However, on micellization, there is a steep increase in the intensity of the solvated NH peak, suggesting that the onset of micellization accumulates some solvated NHs in the bis-amide aggregates. The increase in fluorescence intensity of ANS in the presence of bis-amide and the increase in intensity of the solvated NH stretching band of the bis-amide suggest that, for this bis-amide, the solvophobic groups might be the bis-glycamide heads of the bis-amide, which occupy the interfacial region, and the *p*-phenylenediamine groups occupy the core of the micelles. The micelle structure of the bis-amide is clearly shown in Figure 1b, which is the reverse of class "B" of Chart 1 (see ref 3a), and may be considered as an inverted micelle, since there is no trace amount of water present in the system and the aggregate formation of the bis-amide is in the presence of pure chloroform solvent only.

Aggregation Number of Bis-Amide in Chloroform using Fluorescence Methods. For the determination of aggregation number, pyrene and *N*-cetylpyridinium chloride (CPC) were used as probe and quencher, respectively. Following Turro and Yekta,[19] the aggregation number was determined by measuring the quenching of a micelle-bound fluoro probe by the binding of a quencher using the following expression, which leads to the Poisson distribution[20a]

$$\ln(I_0/I) = N[\mathrm{Q}]/(C_s - \mathrm{cmc}) \qquad (1)$$

where I_0 and I are the emitted light intensities with quencher concentrations zero and [Q], respectively. N and C_s are the mean aggregation number and concentration of the bis-amide, respectively. The technique is subjected to the assumption that the micellar solutions are monodispersed. The validity of the Turro−Yekta model was examined. The micellar aggregation number for 0.5, 1.5, 2.5, and 4 mM bis-amide solutions was calculated from the plot of $\ln(I_0/I)$ vs [Q] (Figure 6). The values of aggregation numbers are found to be 11 ± 1, 21 ± 1, 24 ± 1, and 34 ± 2 for bis-amide concentrations of 0.5, 1.5, 2.5, and 4 mM, respectively. The concentration dependence aggregation

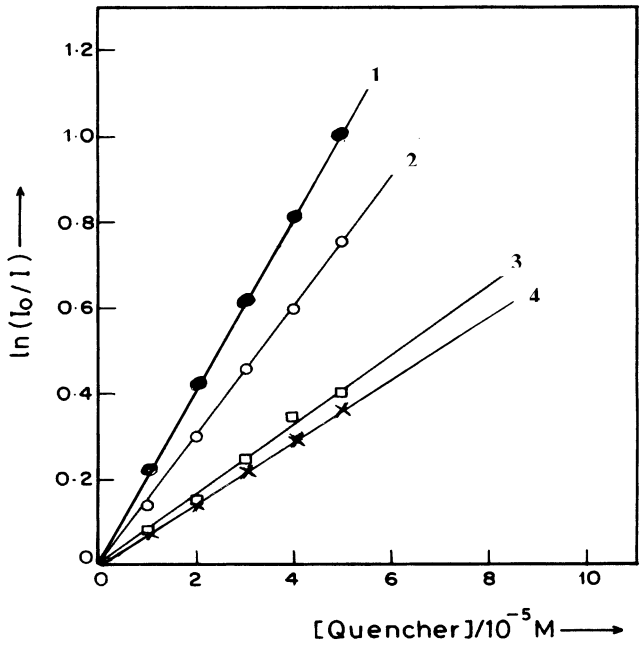

Figure 6. Plots of $\ln(I_0/I)$ vs quencher concentrations in the presence of bis-amide micelles at 22 °C. Curves 1−4: concentrations of bis-amide 0.5, 1.5, 2.5, and 4 mM (fixed), respectively. Conditions: [pyrene] = 1 μM (fixed); λ_{ex} 320 nm; λ_{em} 374 nm.

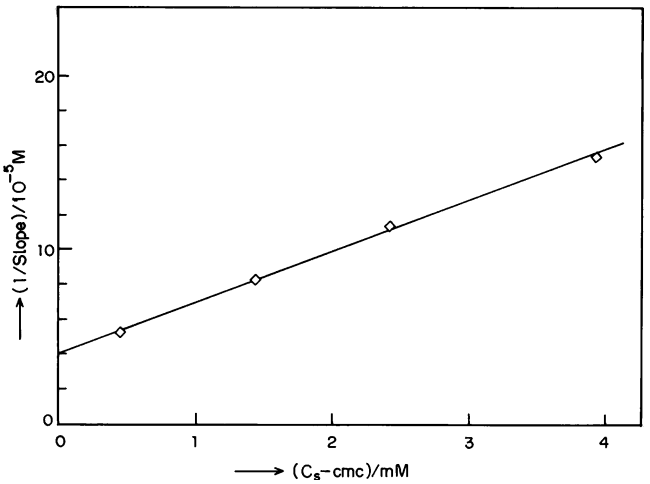

Figure 7. Plot of 1/slope vs C_s − cmc, to determine the mean aggregation number of bis-amide micelles and partition coefficient of the CPC quencher in bis-amide micelles in chloroform (cf. eq 2).

numbers for nonionic heterogeminis, SDS (sodium dodecyl sulfate), and nonionic macromonomer have recently been reported.[11b,c,h,13e,14,21] One of the reviewers has pointed out that the reason the application of eq 1 to our data yields N values that are so different for different bis-amide concentrations is because the Turro−Yekta model handles micellar systems where the probe and the quenchers are fully associated with the micelles. The fact that the plot of $\ln(I_0/I)$ vs [Q] shown in Figure 6 yields such beautiful straight lines indicates that we are right to use such a plot. However, it is important to know how pyrene and CPC partition themselves between the micelles and the bulk (here chloroform). If one assumes that pyrene is solubilized inside the micelles but the quencher partitions itself between the micelles and the solvent with the equilibrium constant (i.e., partition coefficient) K, it can be shown[22] after approximation that

$$1/\text{slope} = (1/K) + (C_s - \text{cmc})/N \qquad (2)$$

TABLE 1: Values of A_2, A_3, and Aggregation Numbers of Bis-Aamide in Chloroform in the Presence of Varying Amounts of Quencher[a]

[bis-amide]/ mM	[quencher]/ 10^{-4} M	$A_2/10^7$	A_3	aggregation no. of bis-amide (N)
1.5	1	−4.208	1.3820	20 ± 3
	2	−4.488	2.6080	19 ± 3
	5	−5.208	7.1826	21 ± 3
4	1	−8.602	1.0815	43 ± 3
	2	−8.892	2.0675	40 ± 3
	5	−9.962	5.0640	40 ± 3

[a] Conditions: [pyrene] = 1 μM (fixed); temperature 20 °C.

TABLE 2: Values of A_2, A_3, and Aggregation Numbers of Bis-Amide Micelles in Chloroform in the Presence of Varying Amounts of Quencher[a]

[bis-amide]/ mM	[quencher]/ 10^{-4} M	$A_2/10^7$	A_3	aggregation no. of bis-amide (N)
1.5	1	−5.6014	1.5026	22 ± 3
	2	−6.6042	2.5023	20 ± 3
	5	−6.6841	6.8023	20 ± 3
4	1	−1.8052	1.1088	44 ± 3
	2	−3.4017	2.0342	41 ± 3
	5	−4.2648	5.2080	41 ± 3

[a] Conditions: [ANS] = 1 μM (fixed), temperature 20 °C.

Here, slope is the slope of the plot of $\ln(I_0/I)$ vs $[Q]_t$ (the total quencher concentration) for the corresponding bis-amide concentration. Now, if 1/slope is plotted against C_s - cmc (see Figure 7), the mean aggregation number ($\tilde{N}$) of the bis-amide micelles and the equilibrium constant of the CPC quencher (K) can be obtained from the slope and intercept, respectively, of the above plot. The mean aggregation number of the bis-amide micelles and the equilibrium constant of the CPC quencher obtained are found to be 31 and 2.5×10^4 M^{-1}, respectively. However, if the probe and quencher are solubilized in micellar aggregates, the following time properties of the luminescence intensities in a generalized decay equation had been reported[20] during the time-resolved fluorescence method, which is based on Poisson distribution:

$$I(t) = I(0)\exp\{-A_2t - A_3[1 - \exp(-A_4t)]\} \qquad (3a)$$

or

$$\ln[I(t)/I(0)] = -A_2t - A_3[1 - \exp(-A_4t)] \qquad (3b)$$

The above equation was fitted to the decay curves using a weighted least-squares procedure. $I(t)$ and $I(0)$ are the emission intensities at time t and zero, respectively. A_2, A_3, and A_4 are constants, which are determined as adjustable parameters. The concentration of the fluoroprobe was kept sufficiently low (1 μM) to prevent excimer or exciplex formation, so that the perturbation of the micellar structure by the probe could be minimized.[20,23] The aggregation number was also calculated using the protocol[20,23]

$$A_3 = [Q]/\{(C_s - \text{cmc})/N\} \qquad (4)$$

As the value of $\exp(-A_4t)$ is very small, it is considered insignificant. Accordingly, the second part of the right-hand side of eq 3b (i.e., within the brackets) had been normalized to 1. The A_2 and A_3 values were obtained from the slope and intercept, respectively, from the plot of $\ln[I(t)/I(0)]$ vs t and are given in Tables 1 and 2. The aggregation numbers for various concentrations of bis-amide micelles along with various concentrations

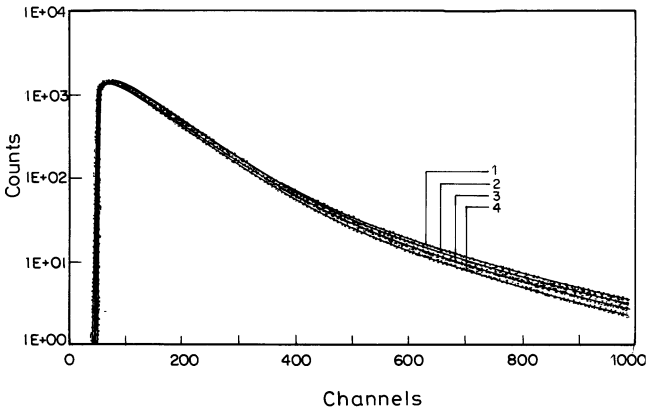

Figure 8. Fluorescence decay curves for pyrene in bis-amide micelles as a function of CPC quencher concentration at 22 °C. Condtions: [pyrene] = 1 μM (fixed); [bis-amide] = 1.5 mM (fixed); λ_{ex} 300 nm; λ_{em} 385 nm. Curves 1−4: [CPC] = 0, 0.03, 0.1, and 0.4 mM, respectively.

of quencher obtained by time-resolved fluorescence methods using pyrene and ANS probes are also depicted in Tables 1 and 2. It has been found that the aggregation numbers obtained by time-resolved methods do not vary significantly with quencher concentrations, irrespective of probes (here, pyrene and ANS) (cf. Tables 1 and 2). However, the aggregation numbers vary with the concentration of bis-amide. For example, the aggregation numbers of 1.5 and 4 mM bis-amide micelles were found to be approximately 20 and 40, respectively (see Tables 1 and 2). Such variation of increasing aggregation numbers with increasing bis-amide concentration has also been observed for the static fluorescence method (cf. Figure 6). It is quite interesting to note that the average value of the aggregation number of the bis-amide micelles for the time-resolved method was found to be 31 (cf. Tables 1 and 2), which was exactly the same as the mean aggregation number obtained in the static fluorescence method using eq 2 (cf. Figure 7).

Overall, the aggregation numbers obtained by the static fluorescence method were in good agreement with those of the time-resolved fluorescence method. It may be mentioned here that the coincidence of aggregation number obtained by static and time-resolved methods is due to the mutual cancellation of the double errors, as pointed out by Tachiya.[20] Although the fluorescence emission intensity of pyrene (1 μM) in chloroform decreases somewhat with the increase in concentration of CPC, even in the absence of bis-amide micelles, the lifetime value does not change significantly in the presence of CPC. The aggregation number of pyrene determined by both static and time-resolved methods was found to be $\ll$1. This indicates that such a low concentration of pyrene (1 μM) in chloroform does not aggregate.

Fluorescence Lifetimes of Pyrene and ANS in Chloroform in the Absence and Presence of Bis-Amide Micelles and the Effect of CPC Quencher. Although the plot of ln[$I(t)/I(0)$] vs t is not shown here, a typical example of the fluorescence decay curves for pyrene (1 μM, fixed) in bis-amide micelles in chloroform using various concentrations of CPC quencher is shown in Figure 8. The measurements were performed on both aerated and deaerated solutions. The decay curves for pyrene in bis-amide micelles, especially at low concentration, were found to be monoexponential in the absence of quencher (cf. Table 3), whereas they were biexponential in the presence of varying concentrations of quencher. However, the contribution of the minor component of pyrene is very low and, hence, shows lower lifetime and relative amplitude values. The lifetimes of

TABLE 3: Fluorescence Lifetimes of Pyrene in Bis-Amide in Chloroform in the Presence of Varying Amounts of Quencher[a]

[CPC]/ 10^{-4}M	A	B*	lifetime (t/ns)	rel amplitude (%)	χ^2
		(a) In the Absence of Oxygen			
0	8.054	0.19471	180 ± 0.1	100	1.24
1	7.212	0.11293	175 ± 0.1	95.46	1.11
		0.64152	5.2 ± 0.02	4.54	
2	9.005	0.18094	170 ± 0.1	96.20	1.27
		0.55002	5.0 ± 0.02	3.80	
3	5.889	0.16206	168 ± 0.1	97.40	1.20
		0.45268	5.0 ± 0.02	2.60	
4	4.2012	0.14201	166 ± 0.1	97.00	1.12
		0.33282	5.0 ± 0.02	3.00	
		(b) In the Presence of Oxygen			
0	−1.946	0.09155	21.71± 0.09	100.00	1.13
1	−0.239	0.01927	19.21± 0.08	93.41	1.07
		0.01240	2.11 ± 0.01	6.59	
2	9.075	0.01108	18.80 ± 0.09	94.02	1.11
		0.01954	2.11 ± 0.01	5.98	
3	5.964	0.01830	18.10 ± 0.06	94.40	1.27
		0.01975	2.11 ± 0.01	5.60	
4	4.380	0.00340	17.60 ± 0.05	95.00	1.24
		0.03332	2.11 ± 0.01	5.00	

[a] Conditions: [pyrene] = 1 μM (fixed); [bis-amide] = 1.5 mM (fixed); temperature 20 °C. Lifetime values of pyrene in chloroform in the absence and presence of oxygen are 220 and 80 ns, respectively.

TABLE 4: Fluorescence Lifetimes of Pyrene in Bis-Amide in Chloroform in the Presence of Varying Amounts of Quencher[a]

[CPC]/ 10^{-4}M	A	B*	lifetime (t/ns)	rel amplitude (%)	χ^2
		(a) In the Absence of Oxygen			
0	3.267	1.98760	170 ± 0.1	93.30	1.10
		0.12025	5.2 ± 0.2	6.70	
1	3.142	1.60723	168 ± 0.2	94.31	1.12
		0.11283	5.0 ± 0.02	5.69	
2	2.982	1.50286	166 ± 0.2	96.28	1.24
		0.08185	4.9 ± 0.02	3.72	
5	2.501	1.42620	164 ± 0.2	97. 00	1.26
		0.06284	4.7 ± 0.02	3.00	
		(b) In the Presence of Oxygen			
0	5.889	2.02194	12.52 ± 0.1	53.16	1.20
		0.13372	0.60 ± 0.02	46.87	
1	4.753	1.26050	11.60 ± 0.2	67.51	1.24
		0.11690	0.50 ± 0.02	32.49	
2	4.341	0.79702	11.53 ± 0.2	75.44	1.23
		0.10920	0.50 ± 0.02	27.45	
5	3.109	1.12887	11.20 ± 0.2	80.12	1.19
		0.20478	0.50 ± 0.02	19.88	

[a] Conditions: [pyrene] = 1 μM (fixed); [bis-amide] = 4 mM (fixed); temperature 20 °C.

pyrene and ANS in bis-amide micelles in chloroform with varying amounts of quencher were obtained from the following reconvolution fit and depicted in Tables 3−6. For the monoexponential curve

$$I(t) = A + B^* \exp(-t/\tau) \quad (5a)$$

and for the biexponential decay curve

$$I(t) = A + B_1^* \exp(-t/\tau_1) + B_2^* \exp(-t/\tau_2) \quad (5b)$$

The lifetime of the major component of pyrene and ANS was slightly decreased with an increase in concentration of the quencher, whereas the lifetime of the minor component of pyrene and ANS does not decrease with the quencher concentration (cf. Tables 3, 4, and 6). Overall, decreased lifetime values

TABLE 5: Fluorescence Lifetimes of Pyrene in Bis-Amide of Varying Concentrations in Chloroform[a]

	lifetime (t/ns)	
[bis-amide]/mM	in the absence of O_2	in the presence of O_2
0	220 ± 0.1	80 ± 0.1
1.5	180 ± 0.1	21.71 ± 0.1
2.5	175 ± 0.1	15.63 ± 0.1
	5.3 ± 0.2	0.55 ± 0.1
4	170 ± 0.1	12.52 ± 0.1
	5.2 ± 0.2	0.60 ± 0.1

[a] Conditions: [pyrene] = 1 μM (fixed); temperature 20 °C. Lifetime values have been presented in the absence and presence of oxygen.

TABLE 6: Lifetime Values of ANS in Bis-Amide Micelles in Chloroform in the Presence of Varying Amounts of Quencher[a]

[bis-amide]/ mM	[quencher]/ 10^{-4} M	A	B*	lifetime (t/ns)	rel amplitude (%)	χ^2
1.5	0	3.8013	0.8020	4.02 ± 0.02	55.30	1.20
			0.2010	0.5 ± 0.02	44.70	
	1	5.6125	0.7018	4.00 ± 0.02	57.30	1.24
			0.1816	0.5 ± 0.02	42.70	
	2	7.2013	0.5320	3.95 ± 0.02	58.28	1.15
			0.1628	0.5 ± 0.02	41.72	
	5	8.2026	0.4320	3.90 ± 0.02	59.42	1.23
			0.1420	0.5 ± 0.02	40.58	
4	0	6.9306	1.4726	3.09 ± 0.02	52.64	1.15
			0.2520	0.5 ± 0.02	47.36	
	1	8.2814	0.9373	3.04 ± 0.02	54.16	1.20
			0.2032	0.5 ± 0.02	45.84	
	2	10.236	0.8876	3.01 ± 0.02	54.76	1.24
			0.1989	0.5 ± 0.02	45.24	
	5	12.256	1.0718	3.00 ± 0.02	54.86	1.25
			0.1385	0.55 ± 0.02	45.14	

[a] Conditions: [ANS] = 1 μM (fixed); temperature 20 °C. The lifetime value of ANS in $CHCl_3$ in the presence of oxygen is 5.94 ns.

with the variation in quencher concentration suggested the dynamic nature of the quenching process. However, the occurrence of partial steady-state quenching may not be ruled out. Moreover, it is pertinent to note that the cmc of CPC in chloroform[24] at 22 °C is 80 mM. In the present investigation, the CPC quencher concentration was kept 200−1000 times lower than that of its cmc. Therefore, the aggregation numbers obtained from both eqs 1 and 4 were for bis-amide micelles in chloroform only; the interference of CPC was minimized. At 293 K, the lifetimes for pyrene in water, chloroform, and *n*-heptane in the absence of oxygen are 190, 220, and 490 ns, respectively.[14,25] The longer lifetime values of pyrene in nonpolar solvents are easily justified. It is well-known[26−28] that the lifetime value of pyrene decreases drastically in the presence of oxygen and with an increase in pressure. At 20 °C and 1 atm, we determined the lifetime values for pyrene in water and chloroform in the presence of oxygen to be 70 and 80 ns, respectively. These values are in good agreement with the literature[26] values. However, it is interesting to note that the above lifetime value of pyrene in chloroform was dramatically decreased to ∼22 ns in the bis-amide micellar aggregates and in the presence of oxygen (cf. Table 3). The experiments have also been performed in the absence of oxygen, and it has been found that the lifetime value of pyrene in bis-amide micellar aggregates (in chloroform) is decreased from 220 to 180 ns (cf. Table 3).

Partitioning of the Probe and Quencher in Bis-Amide Micelles. The above lifetime values for pyrene were further decreased with the increase in CPC quencher concentrations. However, both pyrene and ANS probes have been located in two different regions of the bis-amide micelles, viz. the surface and core of the micelles, even in the presence of CPC quencher environments (cf. Tables 3, 4, and 6). The nature of location of probes in bis-amide micellar aggregates in the absence and presence of CPC quencher environments is similar in both the absence and presence of oxygen. It has been observed that although the lifetime values of the major components of pyrene and ANS were decreased with an increase in concentration of the quencher, the lifetime values of the minor component remained invariant with the quencher concentration (see Tables 3, 4, and 6). Therefore, the accessibility of the fluoroprobe to the CPC quencher in the bis-amide micelles was calculated using the equation

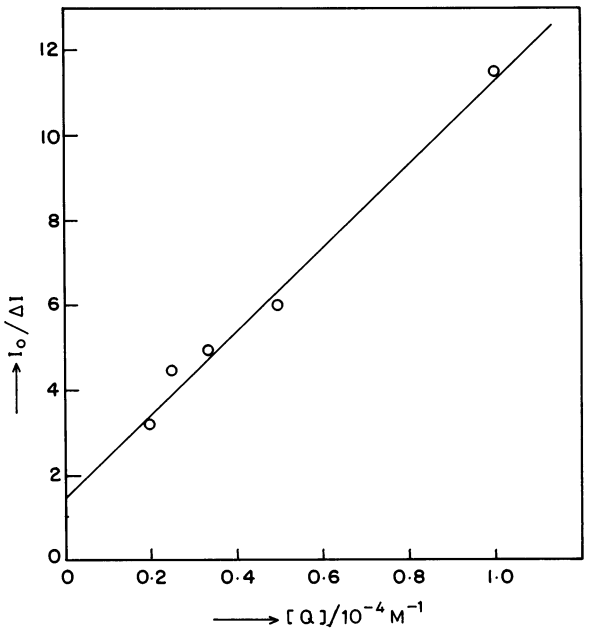

Figure 9. Plot of $I_0/\Delta I$ vs quencher concentration, to estimate the accessibility of the probe to the CPC quencher for pyrene probe (1 μM) in bis-amide micelles (1.5 mM). Conditions: λ_{ex} 320 nm; λ_{em} 374 nm.

$$I_0/\Delta I = 1/f_a + 1/K_{SV} f_a[Q] \quad (6)$$

where I_0 is the emission intensity in the absence of quencher, $\Delta I = I_0 - I$ = difference in emission intensities in the absence and presence of quencher, K_{SV} = Stern−Volmer constant, and f_a = fraction of the fluorescence which is accessible to the quencher. It has been observed that 66% of the total pyrene fluorescence is accessible to quenching and the remaining 34% is not accessible (see Figure 9). Since all the characterizations were made in chloroform, there must be partitioning of pyrene between the micelles and solvent medium so that the added quencher must be accessible to pyrene present in both of the regions of bis-amide micelles in chloroform. We envisaged that 66% of the quenching was observed from the hydrophobic micellar surface (since it is an inverted micelle), which may be due to the major component of pyrene. Normally, highly hydrophobic compounds prefer more hydrophobic sites. Hence, the major portion of pyrene must be solubilized in the hydrophobic micellar surface rather than the solvent medium or in the hydrophilic core and shows a comparatively longer lifetime than the minor component of pyrene, which may be located in the hydrophilic core of the micelles in the present investigation. Similarly, the accessibility of the quencher is also much more prone to the major component than to the minor component, and hence, a decrease in lifetime of the minor

component of pyrene was not observed with an increase in quencher concentration (see Tables 3, 4, and 6). We have also investigated the location of the probe in the nonaqueous bis-amide micelles in the presence of CPC quencher using cyclic voltammetric (CV) techniques.[11f,12c,d,23,29,30] Various electrochemical (EC) probes were used by us in the recent past,[11f,12c,d,29] in order to determine the diffusion coefficient and partition coefficient (K) of the probe in nonmicellar (K_n) and micellar (K_m) phases, respectively. Here, we have used pyrenecarboxaldehyde[30] as an EC probe (instead of pyrene) in bis-amide micelles in the presence of CPC. As the diffusion coefficient is a function of amphipathic (surfactant) concentrations, we have obtained two kinds of partition coefficients, viz. nonmicellar (K_n) and micellar (K_m) phases, and they are 750 ± 30 and 1450 ± 50 M^{-1}, respectively. This suggests that the EC probe is more solubilized in the micellar phase than in the monomeric phase, and the presence of both phases is possible in nonaqueous bis-amide micellar aggregates. The probe partitioning is in good agreement with the quencher accessibility to the fluorescence emission. Cyclic voltammetric and spin−lattice relaxation time measurements[12d] suggested that the partitioning of the probe is highly sensitive to micellar architecture and dynamics of the micelles. For example, although the molecular weight and cmc of both CTAB and CPC are more or less equal, their molecular dynamics and counterion association are totally different; hence, different behaviors of the partition coefficient values were observed in CTAB and CPC micelles.[12d] There is also a possibility of quencher partitioning between bis-amide micelles and solvent. Let us consider a quencher which distributes between the micelles and solvent phases. At nonsaturating concentrations of quencher, the concentrations in the solvent (s) and micellar (m) phases are related by the partition coefficient

$$P = [Q]_m/[Q]_s \tag{7}$$

The total (t) concentration of quencher added ($[Q]_t$) partitions between the solvent and micellar phases according to

$$[Q]_t V_t = [Q]_m V_m + [Q]_s V_s \tag{8}$$

where V represents the volume of the various phases. By defining

$$\alpha_m = V_m/V_t \tag{9}$$

to be the volume fraction of the micellar phase, the apparent quenching constant (k_{app}) can be written as

$$1/k_{app} = \alpha_m[(1/k_m) - (1/k_m P)] + 1/k_m P \tag{10}$$

where k_m is the bimolecular quenching constant for the micelle-bound fluorophore.

When the fluorophore is present in the micellar phase, the apparent quenching constant is dependent upon P, α_m, and k_m. A plot of k_{app}^{-1} vs α_m allows P and k_m to be determined. Thus, the quenching method allows simultaneous quantitation of both the extent to which a quencher partitions into a bis-amide micelles and its rate of diffusion in these micelles. This can be done by a plot of k_{app}^{-1} vs [Q] (see Figure 10). Since the partition coefficient is large, the slope is approximately equal to k_m^{-1}. The intercept is approximately equal to $(k_m P)^{-1}$. From these data one can readily calculate that CPC partitions (7140 ± 20)-fold into the bis-amide micelles. The bimolecular quenching constant k_m was found to be ∼(1.4 ± 0.3) × 10^7 M^{-1} s^{-1}, which is due to collisional quenching by strongly

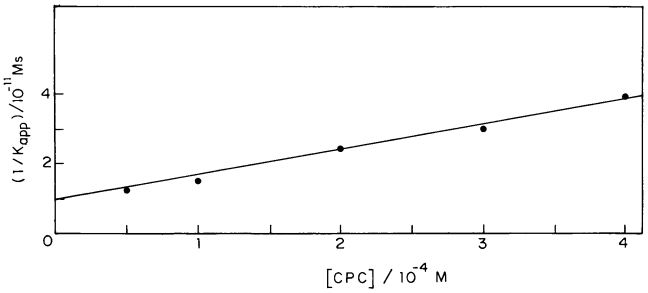

Figure 10. Plot of k_{app}^{-1} vs $[Q]_t$ to determine k_m and P.

partitioning quenchers. For details regarding the estimation of k_m and P, we refer the reader to earlier publications.[28]

The I_1/I_3 plot shown in Figure 2 indicates that pyrene experiences a more apolar environment. It may be that pyrene is not totally solubilized in bis-amide micelles, as some fraction of the pyrene probe could still be in chloroform. To demonstrate that this is not the case, fluorescence decay measurements were acquired at different concentrations of bis-amide micelles above the cmc; the lifetimes of the pyrene and ANS were different from those in chloroform and decreased with an increase in concentration of bis-amide and remained more or less constant in the presence of high concentrations of bis-amide micelles (cf. Tables 3−6). The lifetime of ANS in chloroform has been reported[31] to be 8 ns, but no detailed information was cited. The lifetimes for derivatized ANS with octadecylamine (ANS-AM) both in chloroform solution and in Langmuir−Blogdett (LB) film are less than 8 ns. However, our lifetime results for ANS solutions (1 μM) in chloroform were found to be approximately 6 ns (cf. Table 6). The partition coefficient s(K) of CPC quencher between bis-amide micelles and chloroform obtained by steady-state (using eq 2 and Figure 7) and time-resolved methods (using eq 10 and Figure 10) were found to be 2.5 × 10^4 and 1 × 10^4 M^{-1}, respectively. This high value of K indicates that CPC may be fully associated with the bis-amide micelles in chloroform. It is well-known that dissolved oxygen quenches pyrene fluorescence. The concentration of the dissolved oxygen in water at 1 atm, 1.275 mM, has also been accounted for[28] in addition to CPC quencher. However, in chloroform, the oxygen solubility is higher than that in water. The quenching rate constant k_q^m in bis-amide micelles has also been calculated in the presence of oxygen and found to be (1.2 ± 0.2) × 10^{10} M^{-1} s^{-1}, which is due to a diffusion-controlled reaction. However, the lower k_q value of (2.0 ± 0.5) × 10^9 M^{-1} s^{-1} is somewhat lower than for the diffusion-controlled processes in the absence of oxygen and generally observed in many micellar systems.

Using the biphasic model,[12a] the standard free energy change for micelle formation, ΔG^0_m, has been calculated and found to be −24.3 kJ mol^{-1} at 22 °C. The presence of the negative sign in the free energy of micellization is indicative of spontaneous aggregation.

Two-Dimensional Surface Properties of Bis-Amide Solutions at the Air/Water Interface. Monolayer studies were performed on bis-amide solutions of various concentrations, and the limiting surface areas were plotted against the concentration of bis-amide (Figure 11, inset). A clear break was obtained at the cmc (considered to be dry micelle formation at the interface, as suggested by Israelachvili et al.[7]), which is in good agreement with the results obtained from other techniques: viz., surface tension and UV−visible and fluorescence spectroscopy. The $\pi-A$ isotherms of the bis-amide solutions are shown in Figure 11. The limiting surface area decreases with the increase in concentration of bis-amide, indicating that the bis-amide forms

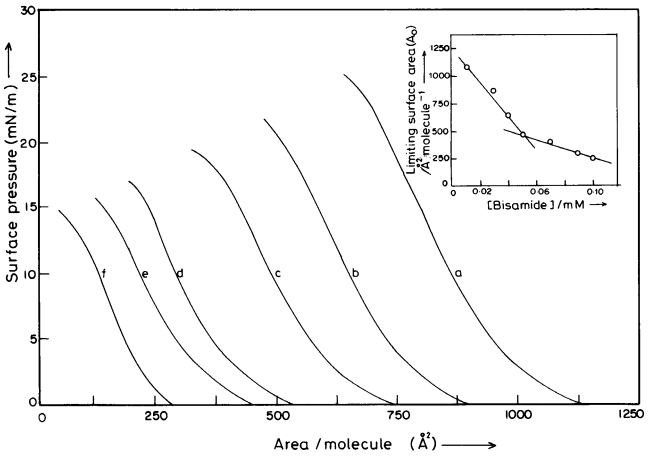

Figure 11. $\pi-A$ isotherms of various concentrations of bis-amide solutions in chloroform at 22 °C. Curves a−f: 0.01, 0.03, 0.04, 0.05, 0.07, and 0.1 mM bis-amide solutions, respectively. Figure inset: limiting surface area (A_0) vs concentrations of bis-amide.

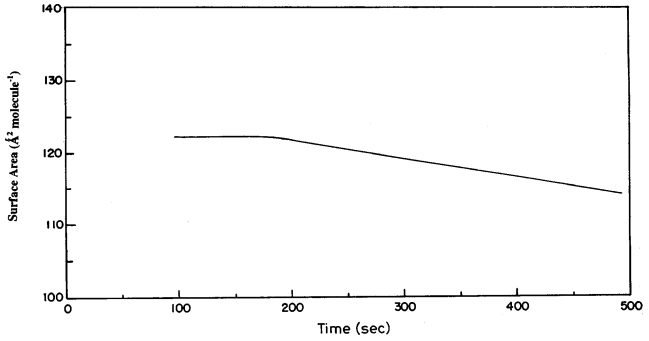

Figure 12. Plot of surface area vs time of films of bis-amide at a constant pressure of 5 mN/m at 22 °C.

a smooth film, and to achieve the low surface areas at the micellar concentration and above, the bis-amide molecules must be folded at the interface. At the two-dimensional air/water interface, the hydrophilic polar moiety embeds into the water phase and hydrophobic groups orient toward the air phase. During compression, the surfactant molecules assemble in an organized structure. Also, the clear break obtained at the cmc indicates that the bis-amide forms a comparatively compact film above the *cmc* and is flexible below the cmc region. Hence, we observed changes in the values of the slope obtained from the plot of limiting surface area vs the concentration of bis-amide. The low values of surface area per molecule indicate the tendency for tight packing. At higher surfactant concentration, the apparent values of area per molecule become very low by the formation of aggregates at the air/water interface. However, due to steric hindrance acting between Boc groups, much rigidity may not be observed, as in the case of the solid condensed state. Hence, we observed a smooth pattern for the pressure−area isotherm, which reveals that the compactness is not as high as we expect in the case of the solid state. The decrease in collapse pressure (π_c) (from 25 to 14 mN/m) with the increase in concentration (from 0.01 to 0.1 mM) (see Figure 11) leads to the conclusion that the film is more stable and flexible even at the low concentration of the bis-amide. The stability of the bis-amide film at higher concentration was also determined by carrying out the monolayer experiment at constant pressure. The plot of surface area vs time of films maintained at a constant pressure of 5 mN/m is shown in Figure 12. The bis-amide films were slightly contracted in the area by 4% with an exposure of 500 s. The surface area remains the same for about 300 s and then dropped down slightly and afterward was constant with time. The possible orientations and packing properties of molecules of a normal conventional surfactant and gemini surfactants at the air/water interface had been presented clearly by Menger et al.[3a] Evidently, our bis-amide gemini surfactant at low concentrations (below cmc) might prefer to lie flat on the water surface, an orientation that would occupy an extraordinarily large surface per molecule. However, when the bis-amide concentration is high (above cmc), there is the possibility of a "horseshoe" conformation,[3] which would place both of the hydrophobic tails into the air and may be separated from another by a distance equal to the length of the spacer[3a] and ultimately occupy a lower surface area per molecule (190−200 Å^2).

Surface Tension and the Gibbs Molecular Area of the Bis-Amide. The plot of surface tension (γ) vs [bis-amide] has already been shown in Figure 3. The plot of γ vs log[bis-amide] has not been shown here. However, the Gibbs molecular area was determined using the equation

$$\Gamma = -(1/2.303nRT)(\mathrm{d}\gamma/\mathrm{d}\log C)_{\mathrm{T}} \qquad (11)$$

$$\text{area} = (N_{\mathrm{A}}\Gamma)^{-1} \qquad (12)$$

where Γ = surface excess concentration, $n = 3$ (constant used by Menger for geminis with flexible spacers; however, in our present case, the spacer is somewhat rigid), $R = 8.314$ J mol^{-1} K^{-1}, T = temperature in Kelvin (here 295 K), γ = surface tension in Newtons per meter, C = concentration in moles per liter, and $N_{\mathrm{A}} = 6.03 \times 10^{23}$ (Avogadro's number). The Gibbs molecular area of the bis-amide was found to be 210 ± 20 Å^2, which is in good agreement with the limiting surface areas obtained for the bis-amide molecule at high concentration (above cmc) during monolayer experiments (Langmuir film balance measurements).

Theoretical Connolly Surface Treatment and Computer Simulation on Bis-Amide. A computer simulation technique using Connolly surface treatment[15] shows that (Figure 13) the contact surface area for the bis-amide molecule is 170 Å^2 (see Table 7), when the bis-amide molecule is in contact with water. The contact surface areas obtained from Connolly surface treatment are in good agreement with the monolayer studies for many systems, viz. hydantoin, porphyrins, Triton X-35, etc., studied recently by us[32] and also in the present investigations. Furthermore, the bis-amide molecules at high concentrations (above cmc) are not in an extended conformation and they may be slightly tilted at the interface, as suggested by Menger. However, the tilted conformation (length 21 Å and breadth 8 Å) is not shown here, whose molecular surface area of 169 Å^2 is in good agreement with the monolayer (well above cmc; Figure 11) and Connolly surface treatments (Table 7). The computer simulation technique also shows that about 11 molecules of bis-amide can aggregate in chloroform to form a cluster (Figure 14), which is in good agreement with the fluorescence studies. The new amphiphilic unimer is interesting, because the difference in solvating a phenylenediamine group or a *tert*-butyloxycarbonyl (*t*-Boc) group should not be very large and could not be directly predicted from the chemical formula. The difference is mediated by the polar bis-glycamide section between the *p*-phenylenediamine and Boc groups. Although the experimental findings indicated the formation of intramolecular hydrogen bonds, the locations of these hydrogen bonds are not shown in Figures 13 and 14. They may be shown where the interaction of these bis-amide micelles with cetyltrimethylammonium bromide (CTAB) micelles will be attempted (in individual and mixed micellar states). In the recent

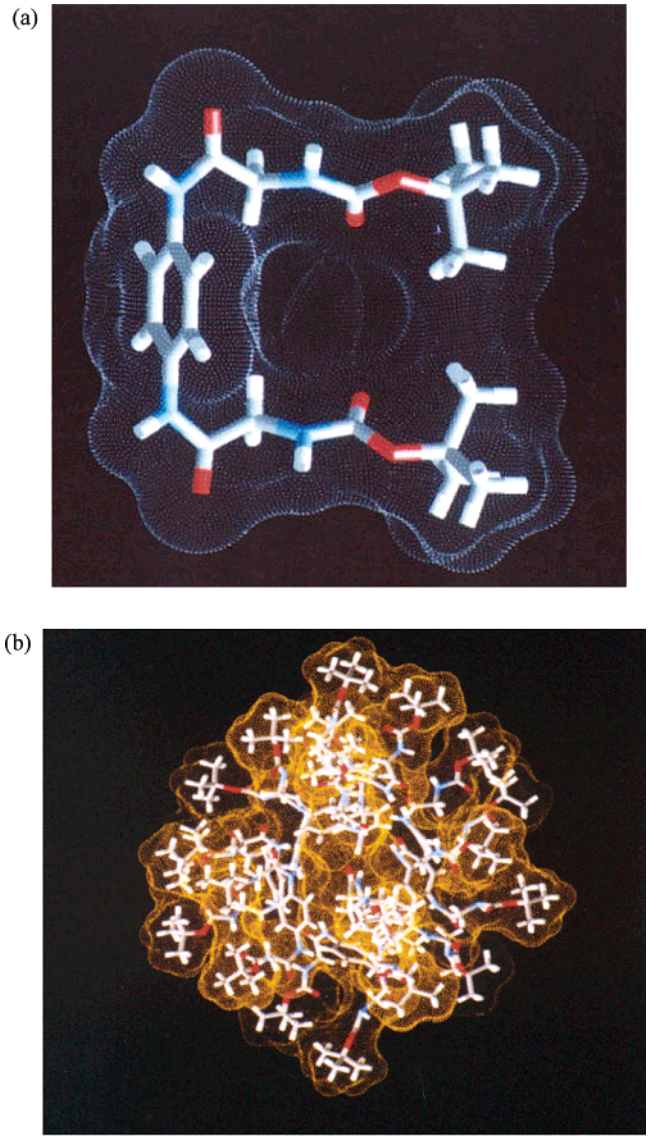

Figure 13. Connolly surface treatment for (a) a bis-amide molecule and (b) its micellar aggregates.

TABLE 7: Surface Areas, Total Areas, and Volume of Single Molecule, Micelle, and Slightly Tilted Conformation of Bis-Amide Using the Connolly Method

	bis-amide		
surface area	single molecule	micelle	tilted conformation
contact (Å^2)	167.96	1201.58	197.97
saddle (Å^2)	193.69	1728.32	199.31
concave (Å^2)	87.44	1397.49	57.04
total area (Å^2)	449.10	4327.38	454.335
volume (Å^3)	463.68	5012.98	417.241

past,[11b,c,h] we have found that the methoxypoly(ethylene glycol)-based macromonomer in aqueous solutions showed two cmc values: one is at 0.1 mM and the other is at 0.2 M. The aggregation numbers of the said macromonomer for primary micellar (<0.2 M) and secondary micellar states were found to be 19 and 95, respectively, and we hypothesized that about five primary micelles of macromonomer can aggregate to form a secondary micelle of macromonomer (which is more prone to polymerization). However, in the present investigation, the occurrence of only one cmc of bis-amide surfactant in chloroform is clearly documented. If we do not consider the averaging procedure of the aggregation number, then the fluorescence results suggest the concentration-dependence aggregation number of bis-amide micelles in chloroform. For example, the aggregation numbers obtained for 0.5, 1.5, 2.5, and 4 mM bis-amide micelles were found to be 11, 22, 25, and 36, respectively. However, one of the reviewers has suggested obtaining a mean aggregation number (using eq 2), and it was found to be 31 for bis-amide micelles during both static and time-resolved fluorescence methods. Another reviewer has suggested that our results clearly demonstrate the micelle formation is of the open association type. Moreover, the simulations were made only for the 11-unit cluster. In this bis-amide structure, the phenylene-diamine groups appear to be assembled around a small hole. This makes sense, because for the large clusters, a hierarchy of association seems to be operative; i.e., in a first step the 11-unit cluster is formed and this establishes the unimer (about 3 or 4 numbers) for further association.

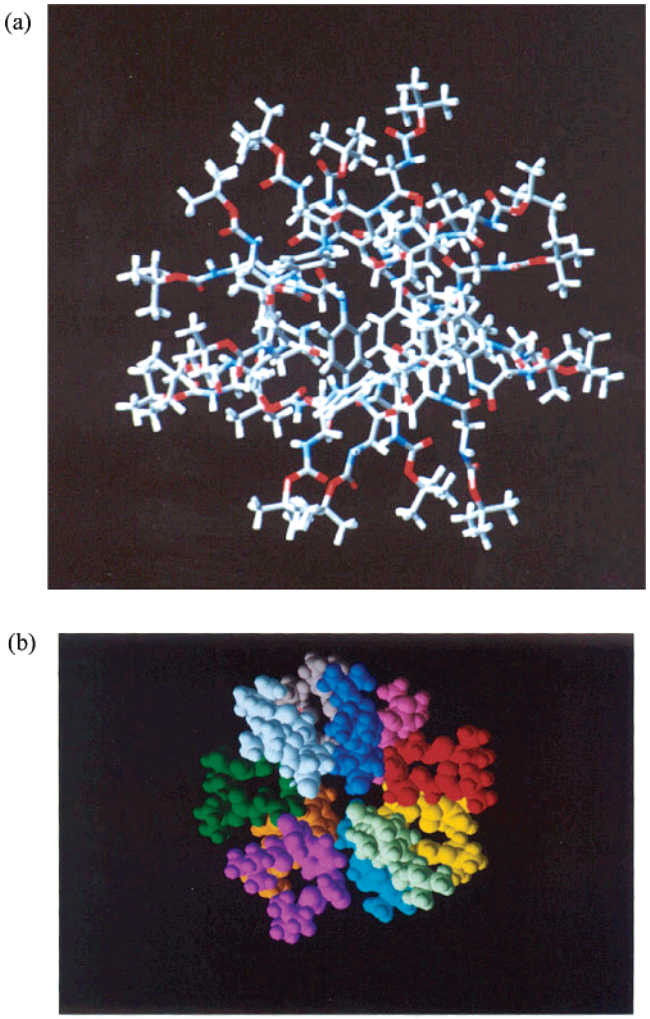

Figure 14. Computer simulation technique, showing that 11 molecules of bis-amide can aggregate to form a cluster: (a) ball-and-stick model of bis-amide aggregates; (b) buckyball structure of bis-amide aggregates.

Conclusion

In conclusion, we established the micelle forming nature of our synthesized unusual nonionic bis-amide gemini surfactant by using various techniques: viz., UV−visible, FT-IR and fluorescence spectroscopy, surface tension, monolayer, and theoretical Connolly surface treatment, including computer simulation techniques. The bis-amide forms a smooth, stable monolayer even at low concentration. The cmc values obtained by various techniques are in good agreement with the results

obtained from Langmuir film balance measurements. The limiting surface areas obtained from monolayer experiments are in good agreement with the contact surface area obtained by Connolly surface treatments. The high value of partition coefficient indicated that the CPC quencher may be fully associated with the bis-amide micelles in chloroform. We do not have the exact data for the partition coefficient (K_m) of pyrene probe in bis-amide micelles in chloroform. However, the K_m value of the pyrenecarboxaldehyde probe in bis-amide micelles in chloroform determined by CV was found to be approximately 1500 M^{-1}. Therefore, there is a possibility that the majority of the pyrene probe may also be fully associated with the bis-amide micelles in chloroform. Fluorescence results suggest that the pyrene probe is located in two regions of the bis-amide micelles: one in the nonpolar surface region and the other in the relatively polar inner core region (as inverted micelles). As the lifetimes of the minor component of pyrene in bis-amide micelles do not change with the addition of CPC quencher, it may be possible that the 34% of the pyrene probe (emission) located in the inner core of the bis-amide micelles is not accessible to the CPC quencher (if it is accessible, then the quenching of emission in the inner region may be due to static quenching). Therefore, full binding of the CPC quencher is in the nonpolar surface region of the bis-amide micelles, where 66% of the pyrene (emission) is located and the corresponding quenching is dynamic. Furthermore, the information obtained from fluorescence quenching, including the lifetime, will prove useful for a variety of studies involving the photochemistry of nonpolar components in micelles.

Acknowledgment. We are grateful to Prof. P. Natarajan, Director, Ultrafast Center, and Dr. P. Ramamurthy, Reader, Department of Inorganic Chemistry, University of Madras, for providing time-resolved fluorescence experimental facilities. Support of research council is also gratefully acknowledged. R.S.G.K. thanks the Council of Scientific and Industrial Research for a fellowship. The technical help of Dr. V. Subramanian in computational techniques is highly appreciated. We are grateful to Prof. R. E. Verrall and Dr. S. Wettig, Department of Chemistry, University of Saskatchewan, for help in writing the computational program to determine aggregation number from time-resolved fluorescence measurements. We are also grateful to anonymous reviewers for their valuable and constructive suggestions.

References and Notes

(1) Huc, I.; Oda, R. *Chem. Commun.* **1999**, 2025.

(2) Huc, I.; Oda, R.; Candau, S. J. *J. Chem. Soc., Chem. Commun.* **1997**, 2105.

(3) (a) Menger, F. M.; Littau, C. A. *J. Am. Chem. Soc.* **1993**, *115*, 10083. (b) Menger, F. M.; Yamasaki, Y. *J. Am. Chem. Soc.* **1993**, *115*, 3840. (c) Menger, F. M.; Keiper, J. S.; Azov, V. *Langmuir* **2000**, *16*, 2062.

(4) Zana. R.; Talmaon, Y. *Nature* **1993**, *362*, 228.

(5) Oda, R.; Huc, I.; Schmutz, M.; Candau, S. J.; Mackintosh, F. C. *Nature* **1999**, *399*, 566.

(6) Zana, R.; Benrraou, M.; Rueff, R. *Langmuir* **1991**, *7*, 1072.

(7) Israelachvili, J. N. *Intermolecular and Surface Forces*, 2nd ed.; Academic Press: London, 1991.

(8) (a) Mandal, A. B.; Jayakumar, R. *J. Chem. Soc., Chem. Commun.* **1993**, 237. (b) Mandal, A. B.; Jayakumar, R. *J. Chem. Soc., Faraday Trans.* **1994**, *90*, 161. (c) Mandal, A. B.; Dhathathreyan, A.; Jayakumar, R.; Ramasami, T. *J. Chem. Soc., Faraday Trans.* **1993**, *89*, 3075. (d) Mandal, A. B.; Jayakumar, R.; Manoharan, P. T. *J. Chem. Soc., Chem. Commun.* **1993**, 853. (e) Jayakumar, R.; Jeevan, G.; Mandal, A. B.; Manoharan, P. T. *J. Chem. Soc., Faraday Trans.* **1994**, *90*, 2725.

(9) Spatz, J. P.; Mobmer, S.; Moller, M. *Angew. Chem.* **1996**, *108*, 1673.

(10) (a) Mandal, A. B.; Ramesh, D. V.; Dhar, S. C. *Eur. J. Biochem.* **1987**, *167*, 617. (b) Rose, C.; Kumar, M.; Mandal, A. B. *Biochem. J.* **1988**, *249*, 127. (c) Rose, C.; Mandal, A. B.; *Int. J. Biolog. Macromol.* **1996**, *18*, 41.

(11) (a) Geetha, B.; Mandal, A. B.; Ramasami, T. *Macromolecules* **1993**, *26*, 4083. (b) Geetha, B.; Mandal, A. B. *Chem. Phys. Lett.* **1997**, *266*, 443. (c) Geetha, B.; Mandal, A. B. *J. Chem. Phys.* **1996**, *105*, 9649. (d) Geetha, B.; Mandal, A. B. *Langmuir* **1995**, *11*, 1464. (e) Geetha, B.; Mandal, A. B. *Langmuir* **2000**, *16*, 3957. (f) Geetha, B.; Mandal, A. B. *Chem. Phys. Lett.* **2000**, *318*, 35. (g) Geetha, B.; Mandal, A. B. *Langmuir* **1997**, *13*, 2410. (h) Geetha, B.; Mandal, A. B. *J. Surf. Sci. Technol.* **2001**, *17*, 29.

(12) (a) Mandal, A. B.; Ray, S.; Moulik, S. P. *Indian J. Chem.* **1980**, *19A*, 620. (b) Mandal, A. B.; Ray, S.; Biswas, A. M.; Moulik, S. P. *J. Phys. Chem.* **1980**, *84*, 856. (c) Mandal, A. B.; Nair, B. U.; Ramaswamy, D. *Langmuir* **1988**, *4*, 736. (d) Mandal, A. B.; Nair, B. U. *J. Phys. Chem.* **1991**, *95*, 9008. (e) Mandal, A. B. *Langmuir* **1993**, *9*, 1932. (f) Mandal, A. B.; Wang, L.; Brown, K.; Verrall, R. E. *J. Colloid Interface Sci.* **1993**, *161*, 292.

(13) (a) Wettig, S. D.; Verrall, R. E. *J. Colloid Interface Sci.* **2001**, *244*, 377. (b) Jenkins, K. M.; Wettig, S. D.; Verrall, R. E. *J. Colloid Interface Sci.* **2002**, *247*, 456. (c) Wettig, S. D.; Verrall, R. E. *J. Colloid Interface Sci.* **2001**, *235*, 310. (d) Wettig, S. D., Ph.D. Thesis, University of Saskatchewan, 2000. (e) Alami El-Ouafi., Ph.D. Thesis, Chalmers University of Technology, 2002.

(14) (a) Kanthimathi, M,; Deepa, K.; Nair, B. U,; Mandal, A. B. *Bull. Chem. Soc. Jpn.* **2000**, *73*, 1769. (b) Krishnan, R. S. G.; Thennarasu, S.; Mandal, A. B. *Chem. Phys.* **2003**, *201*, 195.

(15) (a) Connolly, M. L. *Science* **1983**, *221*, 709. (b) Connolly, M. L. *J. Appl. Crystallogr.* **1983**, *16*, 548.

(16) Slavik, J. *Biochim. Biophys. Acta* **1982**, *694*, 1.

(17) (a) Gilson, M. K.; Hanig, B. H. *Nature* **1987**, *330*, 84. (b) Dao Pin, S.; Liao, D. I.; Remigton, S. J. *Proc. Natl. Acad. Sci. U.S.A.* **1989**, *86*, 5361.

(18) (a) Toniolo, C.; Bonoja, G. M.; Salardi, S. *Int. J. Biol. Macromol.* **1981**, *3*, 377 (b) Baron, M. H.; Beloze, C.; Kasman, G. D. *Biopolymers* **1978**, *17*, 2225.

(19) Turro, N. J.; Yekta, A. *J. Am. Chem. Soc.* **1978**, *100*, 5951.

(20) (a) Infelta, P.; Gratzel, M.; Thomas, J. K. *J. Phys. Chem.* **1974**, *78*, 190. (b) Tachiya, M. *Chem. Phys. Lett.* **1975**, *33*, 289. (c) Tachiya, M. *J. Chem. Phys.* **1983**, *78*, 5282. (d) Infelta, P. P.; Gratezel, M. *J. Chem. Phys.* **1983**, *78*, 5280.

(21) Bales, B. L.; Almgren, M. *J. Phys. Chem.* **1995**, *99*, 15153.

(22) Yekta, A.; Aikawa, M.; Turro, N. J. *Chem. Phys. Lett.* **1979**, *63*, 543.

(23) (a) Zana, R.; Mackay, R. A. *Langmuir* **1986**, *2*, 109. (b) Zana, R., Ed. *Surfactant Solutions, New Methods of Investigations*; Marcel Dekker: New York, 1987; Chapter 5.

(24) Bag, N.; Dhathathreyan, A.; Mandal, A. B.; Ramasami, T. *J. Porphyrins Phthalocyanins* **1998**, *2*, 345.

(25) Zachariasse, K. A,; Kuhnle, W.; Leinhos, U.; Keynders, P.; Striker, G. *J. Phys. Chem.* **1991**, *95*, 5476.

(26) Gong, Y. K.; Nakashima, K. *Chem. Commun.* **2001**, 1772.

(27) Alargova, R. G.; Kochijashky, I.; Zana, R. *Langmuir* **1998**, *14*, 1575.

(28) Lakowicz, J. R., Ed. *Principles of Fluorescence Spectroscopy*; Plenum Press: New York, 1983; Chapter 9.

(29) Mandal, A. B.; Nair, B. U. *J. Chem. Soc., Faraday Trans.* **1991**, *87*, 133.

(30) Verrall, R. E.; Milioto, S.; Giraudeau, A.; Zana, R. *Langmuir* **1989**, *5*, 1242.

(31) Diamandis, E. P. *Clin. Biochem.* **1988**, *21*, 139.

(32) (a) Krishnan, R. S. G.; Thennarasu, S.; Mandal, A. B. Submitted for publication in *Phys. Rev. Lett.* (b) Mandal, A. B.; Srividya, N.; Wolff, T. To be submitted for publication in *Langmuir*.